

A New Look at Open Cluster NGC 6520

Andrew P. Odell

Dept of Physics and Astronomy, Northern Arizona University, Flagstaff AZ 86011

Andy.Odell@nau.edu

ABSTRACT

We use CCD and photoelectric photometry with Strömgren filters along with medium resolution spectra to investigate NGC 6520, an open cluster very nearly in the direction of the galactic center. We find an age of 60 Myr, a distance of 2 kpc, and an average reddening $E(b-y) = 0.295$, but which increases toward the south. The average heliocentric radial velocity of the B stars is -29 km s^{-1} , while the velocity of the nearby Barnard 86 is about 0 (heliocentric, -11 km s^{-1} compared to the LSR). This velocity difference amounts to about 1.8 kpc since the cluster formed, implying that it is extremely doubtful NGC 6520 is related to Barnard 86.

Subject headings: open clusters: general – open clusters: individual(NGC 6520)

1. Introduction

The young open star cluster NGC 6520 (C1800-279) has been neglected, mostly because it appears in a crowded field only four degrees from the Galactic center (see Fig. 1). The most recent study of the cluster, by Carraro et al. (2005), derived an age of 150 ± 50 Myr (million years) and distance of 1.90 ± 0.1 kpc. These authors noted that the nearby dark nebula Barnard 86 has a distance consistent with that of the cluster, and that the nebula overlaps the cluster. They made the hypothesis that the two objects are related - that Barnard 86 is perhaps the cluster's birth cloud, which has become generally accepted. This is puzzling, as it is thought that the mean lifetime of molecular clouds is ≈ 10 Myr (Blitz & Shu 1980).

Hayford (1933), in a study of Galactic rotation, published spectral types (from Trumpler) and radial velocities for three stars in NGC 6520. Merrilliod et al. (2008) superseded that work with velocities for the three late type supergiants.

Zug (1937), in a followup study to Hayford, listed photographic magnitudes and color indices for 50 stars, along with spectral types (also from Trumpler) and color excesses for nine stars. The existence of early B and possibly even an O star in the cluster argued for a very young age. Houck

(1957) was analyzing a color-magnitude diagram (CMD) of the cluster, but the results were evidently never published. Houck pointed out that there were three evolved supergiants in the direction of the cluster, which is rather unusual.

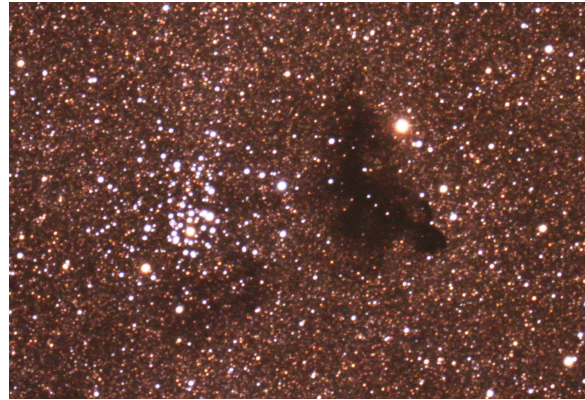


Fig. 1.— An image taken by Klaus Brasch showing NGC 6520 and Barnard 86. North is up, east to the left. Note the patchy extinction visible to the south of the cluster.

Svolopoulos (1966) produced a photographic CMD for NGC 6520, deriving a distance of 1.65 kpc and age of 800 Myr with a reddening estimate for $E(B-V)$ of 0.27. Lindoff (1968) estimated a distance and age of 1.7 kpc and 54 Myr

from relative numbers of stars on the upper main sequence, based on Zug's (1937) data. Santos Jr & Bica (1993) use integrated spectrophotometry continuum levels and line strengths to estimate reddening of $E(B-V)=0.56$ and the low age of ≈ 50 Myr for NGC 6520.

The first believable photometry for NGC 6520 was done by Kjeldsen & Frandsen (1991) who used a CCD with UBV filters; they derive a distance of 1.6 kpc, a mean $E(B-V)$ of 0.43, and they estimate the age to be 190 Myr; they note that the extinction could be variable over the cluster (which we confirm here). Carraro et al. (2005) use this reddening value, as they did not obtain photometry in the U filter. These disparate ages motivated the current study, which concludes that the cluster is younger than most previous estimates.

NGC 6520 was featured on the cover of the NOAO/NSO Newsletter September 2009 issue, with a comment that it '...probably formed from gas related to the nearby dust cloud.' We find here that the cluster and the dust cloud were almost certainly not near each other when the cluster formed, even if they might be now.

2. Observations

2.1. Photometry

NGC 6520 never rises above two airmass in Arizona and an inadequate set of standards was observed during the CCD observations discussed below. Therefore, calibration was done with photoelectric photometry (PE) from five nights in 1997 (UT June 29, 30 and July 1) and 1998 (UT July 1 and 2) using the White photometer with Strömgren uvby filters on the Lowell Observatory 0.8m telescope. Over 20 Strömgren standard stars were used each night, and a total of 22 target stars were observed on at least two of the nights. These targets were chosen on the basis of appearing single on preliminary CCD images, and with a range of color.

All five nights were extremely constant, photometric to within about 0.006 mag. The calibration and reduction to standard magnitudes were done for each night using the PHOTCAL package of IRAF¹, specifically the fitparams and evalfit tasks;

color indices were used and a color term was included, and full documentation is available at the end of the longform of Table 1. These magnitudes were used to further calibrate the CCD images as described next.

Multiple CCD images of NGC 6520 were obtained with the Steward Observatory 1.52m Kuiper telescope on UT April 3, 2000 using Strömgren uvby filters with the BigCCD 4K camera (binned 4x4 to give a field 12' square and pixel size 0.7"). The total exposure times were respectively 480, 480, 120, and 50 seconds in four or more images (to eliminate cosmic rays); twilight flats were used. Eight Strömgren standard stars were observed, which were not adequate for good calibration, so PE as described above was added to the calibration.

The CCD images were reduced in the standard way using IRAF, and the individual frames were combined. Aperture photometry was done with IRAF task phot and the same aperture as for the PE data. This allowed the PE cluster members to be used to derive the transformation to standard Strömgren magnitudes (included at the end of the longform of Table 1) using the IRAF PHOTCAL tasks fitparams and invertfit.

Final magnitudes were then extracted from each of the four combined images using DAOPHOT in IRAF and corrected to the standard system. The standard colors thus formed are listed in Table 1 cols 4-7 (V (derived from y), $(b-y)$, m_1 , and c_1). IRAF formal errors are less than 0.04 mag for all colors of the B stars (and usually much smaller), and 0.02 mag in b and y for the A stars. Missing values of m_1 and c_1 are due to large formal errors in the faint, red stars. Dereddening is described in section 3.

2.2. Spectroscopy

To better judge cluster membership, we obtained spectra of 30 stars near the cluster center on UT July 7, 2012, and a second set of spectra for nine of those on July 8 with the B&C spectrograph on the Steward Observatory 2.3m Bok telescope. The second night was hampered by clouds, and the fact that good wavelength calibration was not available precludes radial velocities. Spectra were also obtained for spectral standard stars. The spectrograph configuration was such as

¹IRAF is distributed by NOAO, which is operated by AURA under agreement with the National Science Foundation

to produce 1.35Å (two pixel) resolution, using the 832/mm grating in second order and a slit width of 1.5''. Wavelength coverage was about 3865Å to 4710Å. The spectra were reduced with IRAF and radial velocities were obtained with task fxcor. The IRAF task rvidlines was used to derive the velocities of τ Her (-1.0 km s⁻¹) and Zug 2 (-28.6 km s⁻¹), the templates for B stars and later types, respectively.

Spectral types and radial velocities are given in Table 1, columns 11 and 12 respectively. The fxcor uncertainty in velocity is about 10 km s⁻¹ for the B stars, and slightly smaller for later types. Binarity is common among B stars; Chini et al. (2012) find about 35% binaries among B4-B6 and 20% among B7-B9 stars. With only one velocity for each case, we cannot identify individual binaries, but undetected companions will have an effect on velocities tabulated here. In column 13, the letter N indicates the star may not be a cluster member, as discussed in section 3.3.

Zug 2, 3, and 4 were included in the cluster RV program by Mermilliod et al. (2008), who find -23.13, -24.12, and -23.41 km/sec, respectively. The values found here are -28.6, -32.5, and -23.5 km/sec, in reasonable agreement. Our mean cluster velocity is also consistent with the average velocity of the cluster given by Hayford (1933) of -26 km s⁻¹, which was based on two spectra each of three stars, all having different values for the two spectra (i.e. likely binaries).

3. Analysis

3.1. Extinction

De-reddening was done using the relation for unreddened B stars given in Crawford et al. (1970) $(b-y)_0 = -0.116 + 0.097c_1$ by iterating in the following manner. Based on the measured c_1 , a preliminary $(b-y)_0$ was calculated with that equation. That $(b-y)_0$ allowed for a preliminary color excess $E(b-y) = (b-y) - (b-y)_0$ to be found. The extinction to c_1 is $E(c_1) = 0.2E(b-y)$ which allows a better $c_1 = c_1 - E(c_1)$ to be calculated, and used in the first equation above to get an improved $(b-y)_0$; this is iterated until no further change occurs. The de-reddened $(b-y)_0$ and V_0 are given in Table 1, cols 8 and 9, and the color excess $E(b-y)$ is given in col 10.

A least-squares plane fit of $E(b-y)$ vs RA and

dec shows extinction decreasing eastward at a rate of -0.71 mmag per RA second, or -2.5 mmag per arcminute, and increasing southward by 10.9 mmag per arcminute of dec. This is shown in Fig. 2, the derived $E(b-y)$ for B stars as a function of position on the sky (*i.e.* a 3-D plot).

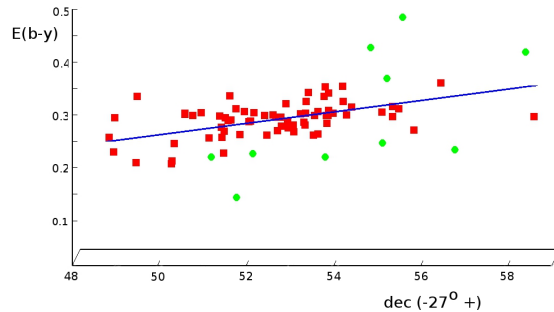


Fig. 2.— Color Excess $E(b-y)$ in magnitudes for NGC6520 B stars (red squares) and probable non-members (green circles, not used in fit) as a function of declination in arcminutes south from -27° . The (blue) line is the fit of a plane to the members. The third axis of this 3-D plot is Right Ascension looking east into the page, from $18^h03^m00^s$ to $18^h03^m50^s$. The tilt of the RA axis has been chosen so that the reader is viewing the plane edge-on; this tilt is so slight that the RA values have been omitted from the third axis for lack of space in the figure.

Thus most of the extinction variation is in the north-south direction, even though Barnard 86 is located to the west. This makes it unlikely that much or any of the extinction at the cluster is due to that cloud. In an image of the cluster (see Fig. 1), it is easy to see patchy clouds of dust in line with the southern border of the cluster, and thus the scatter in Fig. 2 is not unexpected, especially to the right. The figure also shows some outlier stars where the extinction is anomalous and may be indicating these are not cluster members; see section 3.3.

For stars later than B, the above method will not work to find extinction, so a least-squares fit of a plane was made to the extinction as a function of RA and dec for the B stars. This fit was used to correct for extinction for later type stars in Table 1, and for these stars, the $E(b-y)$ extinction in column 10 is marked with an asterisk

(*). Since the extinction is patchy, we expect this to give rise to substantially more scatter in the dereddened colors for the later type stars.

3.2. Color Magnitude Diagram

A color-magnitude diagram (CMD) is an excellent diagnostic tool to determine age and distance for a star cluster. Columns 8 and 9 ($(b - y)_0$ and V_0) of Table 1 are plotted in Fig. 3, with different symbols for B stars dereddened individually, and the A stars and supergiants dereddened by a plane fit to the reddening. As expected, the scatter for the B stars is much less than for the A stars.

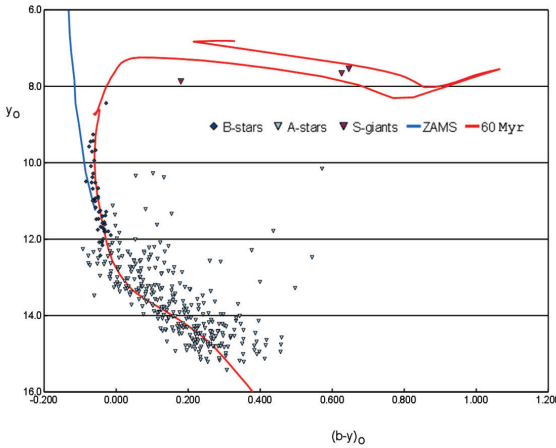


Fig. 3.— The CMD for NGC 6520, showing V_0 vs $(b - y)_0$. Included are the ZAMS and the 60 Myr isochrones, adjusted to a distance modulus of 11.5.

Also plotted are two isochrones², lines of constant age, for stellar evolution models as described by Marigo et al. (2008). The isochrones provide the uvby Strömgren magnitudes for various mass stars at a chosen age and metallicity. There are only a few adjustable parameters needed to fit the observed points, and so the age and distance that best represent the cluster can be determined. The other parameter, metallicity, is chosen to be typical of recent star formation, $Z=0.019$. Various ages were chosen, and the one that fit reasonably well is 60 Myr. The B stars on the upper main sequence, for which reddening is well determined, are the prime ones to fit for age. Further down the main sequence, in the region of the A

stars, the isochrone can be adjusted up and down to fit the observed points by converting absolute magnitudes to the measured apparent magnitudes, adding a distance modulus, which is determined to be about 11.5, implying a distance of 2 kpc. The two G supergiants, Zug 3 and 4, are very close to the blue loop in the isochrone.

The primary cause of uncertainty in the age and distance comes from the variable and patchy reddening. However, the spectral types of the B stars indicate that the age of 60 Myr cannot be too far from correct; the earliest type is B4 V, indicating a mass of about $6M_\odot$, which would have a main sequence lifetime of about this age. It is unlikely that additional observations can improve the CMD analysis.

Fig. 4 is a CMD based on $(v - y)_0$ rather than $(b - y)_0$. The range of this color is larger, and might be more discriminating of the age and distance to the cluster. In this case, it can be seen that the age might be slightly greater than 60 Myr, and the best fit of the distance modulus is about 11.2, for a distance of 1.7 kpc.

We note here that the difference between our age and that of Carraro et al. (2005) arises from their exclusion of B stars farther than $30''$ from the cluster center. Our radial velocities show these stars to almost certainly be cluster members; they are the brightest, bluest stars in the cluster. Further, dereddening individual B stars substantially decreases the scatter in our B star measurements.

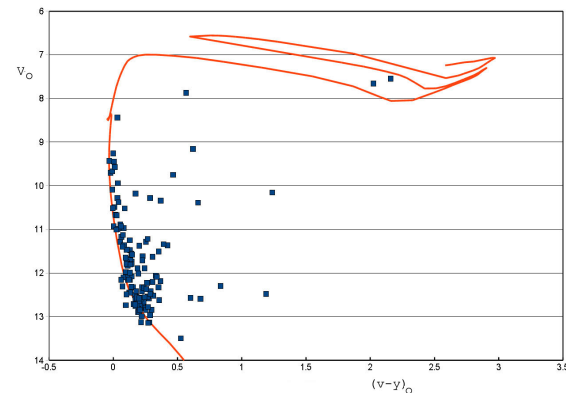


Fig. 4.— The CMD for NGC 6520, showing V_0 vs $(v - y)_0$. Included is the 60 Myr isochrone, adjusted to a distance modulus of 11.20.

²(available at <http://stev.oapd.inaf.it/cmd>)

3.3. Cluster Membership

There are several potential indicators in the data described here which could indicate cluster membership, such as radial velocity, extinction, strength of the CaII K line (for the B stars), position in the CMD, and/or distance from the cluster center (here taken to be $18^h03^m25^s$, $-27^\circ53'40''$). The stars that are most interesting in this regard are as follows.

Zug 1 (=HD164621) is classified as a B9 III. It is rather far from the cluster center, about $4'$ west. Its extinction is the lowest of any B star in the cluster, $E(b - y) \approx 0.14$, where the average is about 0.27 mags at its dec. The CaII line has an equivalent width of about 0.6\AA , whereas the typical B star in the cluster is more like 0.3\AA . The radial velocity is about -25 km s^{-1} , similar to the average of the other B stars in the cluster of -29 km s^{-1} . This being the brightest star in the cluster, it would be valuable as an age indicator, but not essential; it lies about a half-magnitude below the 60 Myr isochrone. Taken together, all this indicates the star may not be a cluster member.

Zug 2 (=HD164654, Hayford 1) is an F4 or F5 Ib star located about an arc minute from the cluster center. The extinction and Ca II line cannot indicate anything about cluster membership. Its radial velocity is -28.6 km s^{-1} , near the cluster average. This star's position in the CMD is also about a half magnitude below the first crossing to the red with a hydrogen burning shell. This crossing is quite fast, so it would be unlikely to catch a star in this phase, but not impossible.

Zug 3 (=HD164684) and Zug 4 (=CD-27 12315) are both G8 I spectral type, the former about two arc minutes southeast of the cluster center, the latter within a few arc seconds. Their radial velocities are -44 and -36 km s^{-1} , both close to the average. They both lie on the blue loop of the CMD, indicating they are in the core helium burning phase.

There are several other, less important stars that are probably not cluster members, based on radial velocity and extinction; they are indicated in column 10 of Table 1.

4. Conclusions

We find NGC 6520 to be quite a bit younger than most previous estimates, i.e. about 60 ± 10 Myr, consistent with stars of spectral type B4 and B5 in the cluster (Negueruela & Marco 2012). Its distance of about 2 ± 0.2 kpc (putting it on the outer edge of the Scutum-Centaurus spiral arm (Churchwell et al 2009)) has been reasonably estimated, but the distance to Barnard 86 has never been measured. Under the assumption that Barnard 86 is at the same distance as the cluster, Carraro et al. (2005) found its properties to be reasonable, but this is hardly proof.

They also measured a radial velocity of $+11 \text{ km s}^{-1}$ compared to the local standard of rest, which is consistent with that estimated by Clemens & Barvainis (1988). This translates into roughly 0.0 km s^{-1} heliocentric velocity. Table 1 col. 12 lists the heliocentric radial velocities of stars for which we obtained spectra; the typical velocity is about -30 km s^{-1} .

The main conclusion here is that the cluster and cloud have different heliocentric radial velocities by about 30 km s^{-1} . This, in the 60 Myr the cluster has been in existence, amounts to about 1.8 kpc relative motion, and would be greater if the cluster were older. So, if the two objects are at the same distance today, they were not at the time the cluster formed, and thus almost certainly have nothing to do with each other. Other problems with this idea include no known mechanism for ejecting an entire cluster from its birth cloud at that speed, and an ejection radially outward through the galaxy, but with essentially no tangential velocity. We conclude NGC 6520 was not formed in Barnard 86.

It is possible that VLBI radio observations could establish a heliocentric parallax for Barnard 86, which would be interesting to determine its location and pin down some of its characteristics.

I thank Steward and Lowell Observatories for allocating telescope time for this project. I appreciate many useful discussions with Brian Skiff, and correspondence with Daniel Majaess and Giovanni Carraro, as well as many useful comments from an anonymous referee. This work made use of the SIMBAD database, operated at CDS, Strasbourg, France.

I would like to dedicate this paper to the memory of Dr. Theodore E. Houck, who taught me to be careful in everything I do.

Facilities: LO:0.8m (White photometer), SO:Kuiper (BigCCD), Bok (B&C Spectrograph)

REFERENCES

- Blitz, L. & Shu, F. H. 1980, ApJ, 238, 148
- Carraro, G., Méndez, R. A., May, M., & Mar-dones, D. 2005, AJ, 130, 635
- Chini, R., Hoffmeister, V. H., Nasseri, A., Stahl, O., & Zinnecker, H. 2012, MNRAS 424, 1925
- Churchwell, E., Babler, B. L., Meade, M. R., Whitney, B. A., Benjamin, R., Indebetouw, R., Cyganowski, C., Robitaille, T. P., Povich, M., Watson, C., & Bracker, S. 2009, PASP 121, 213
- Clemens, D. P., & Barvainis, R. 1988, ApJS, 68, 257
- Crawford, D. L., Glasby, J. W., & Perry, C. L. 1970, AJ, 75, 822C
- Hayford, P. 1933, Lick Obs. Bull., 16, 119
- Houck, T. E. 1957, AJ, 62 No. 1253, p 318 Observatory Reports, University of Wisconsin
- Kjeldsen, H., & Frandsen, S. 1991, A&AS, 87, 119
- Lindoff, U. 1968, Arkiv for Astron., 5, 1
- Marigo, P., Girardi, L., Bressan, A., Groenewegen, M.A.T., Silva, L., & Granato, G.L. 2008, A&A, 482, 883
- Mermilliod, J. C., Mayor, M. Udry, S. 2008 A&A, 485, 303
- Negueruela, I. & Marco, A. 2012, AJ, 143, 46
- Santos J.F.C. & Bica E. 1993, MNRAS, 260, 915
- Svolopoulos, S. N. 1966, Z. Astrophys., 64, 67
- Zug, R. S. 1937, Lick Obs. Bull., 18, 89

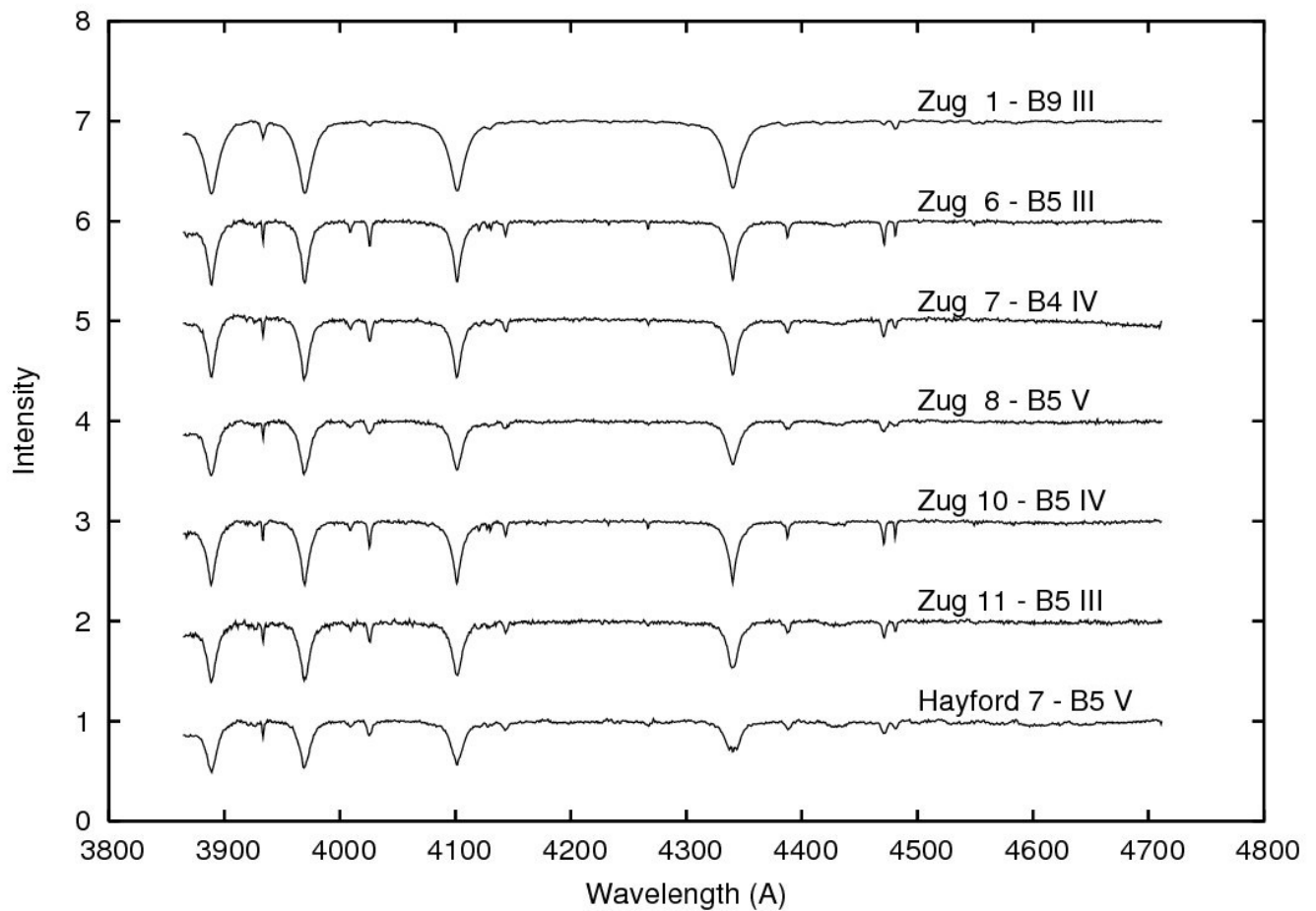


Fig. 5.— Spectra of seven of the earliest and most interesting B stars in NGC6520.

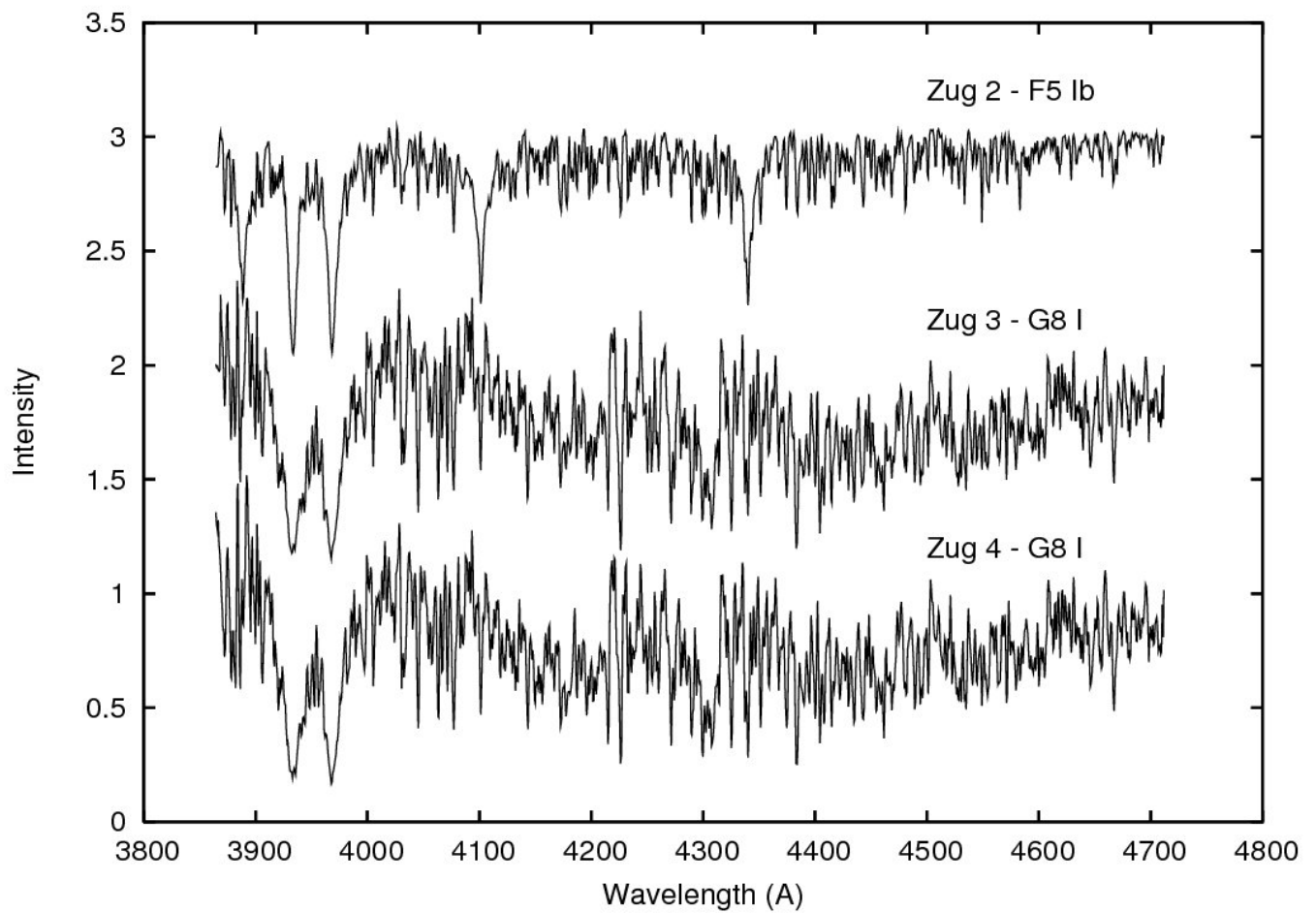


Fig. 6.— Spectra of the three late-type supergiants in NGC6520.

TABLE 1
NGC6520 PHOTOMETRY AND SPECTROSCOPY RESULTS

Zug No.	RA	dec	V	(b-y)	m_1	c_1	$(b - y)_o$	V_o	$E(b - y)^a$	Sp T	RV	Notes ^b
	(18 ^h 03 ^m +)		(-27 ^o +)								(km s ⁻¹)	
1	12.0	51 45	9.038	0.111	0.044	0.931	-0.028	8.439	0.139	B9 III	-25	N
2	22.2	52 55	9.078	0.461	0.118	1.516	0.180	7.869	0.281*	F5 Ib	-29	
3	30.8	54 44	8.820	0.943	0.771	0.084	0.646	7.544	0.297*	G8 I	-32	
4	24.8	53 27	8.887	0.912	0.682	0.280	0.626	7.658	0.286*	G8 I	-24	
5	27.5	51 21	10.301	0.178	0.050	0.587	-0.064	9.261	0.242	B8 V	-41	
6	31.0	53 27	10.655	0.210	0.057	0.520	-0.071	9.447	0.281	B5 III	-26	
7	23.0	52 50	10.757	0.245	-0.002	0.597	-0.064	9.428	0.309	B4 IV	-28	
8	11.3	53 18	10.919	0.215	0.024	0.564	-0.067	9.707	0.282	B5 V	-35	
9	22.2	52 06	10.932	0.236	0.012	0.663	-0.057	9.670	0.293	B7 V	-34	
10	24.8	52 51	11.261	0.203	0.045	0.532	-0.070	10.088	0.273	B5 IV	-34	
11	21.6	53 21	11.366	0.270	0.052	0.630	-0.061	9.941	0.331	B5 III	-22	
12	38.3	52 00	11.367	0.120	0.112	0.370	-0.084	10.490	0.204	B8 V	-25	N
13	27.1	53 33	11.532	0.227	0.067	0.599	-0.064	10.283	0.291	
14	15.0	51 27	11.499	0.323	0.175	0.914	0.054	10.343	0.269*	F8 V	-31	N
15	17.2	51 22	11.668	0.200	0.047	0.549	-0.068	10.516	0.268	B6 V	-21	
16	25.0	53 05	11.598	0.414	0.303	0.849	0.133	10.388	0.281*	G8 V	+25	N
17	22.9	53 18	11.865	0.255	0.104	0.661	-0.058	10.519	0.313	B8 V	-51	
18	26.2	52 38	12.034	0.198	0.037	0.649	-0.058	10.933	0.256	
19	27.8	53 00	12.061	0.191	0.098	0.603	-0.062	10.971	0.253	
20	25.2	54 08	11.841	0.274	0.065	0.586	-0.066	10.380	0.340	
21	26.3	53 16	12.130	0.239	0.063	0.734	-0.050	10.886	0.289	
22	29.5	51 05	12.123	0.159	0.152	0.786	-0.044	11.251	0.203	N
23	29.6	55 01	12.210	0.225	0.116	0.605	-0.063	10.972	0.288	
24	15.2	53 57	12.269	0.232	0.070	0.590	-0.065	10.994	0.297	
25	22.8	52 01	12.116	0.226	0.072	0.736	-0.050	10.929	0.276	B8 V	no RV	
26	42.5	54 53	11.411	0.864	0.572	10.155	0.292*	
27	34.2	55 00	12.456	0.172	0.167	0.673	-0.055	11.479	0.227	N
28	32.9	51 16	12.573	0.248	0.174	0.945	-0.030	11.379	0.278	
29	24.1	51 04	12.331	0.195	0.073	0.751	-0.048	11.287	0.243	
30	24.6	53 48	12.438	0.238	0.083	0.668	-0.057	11.170	0.295	B8	-36	
31	32.6	55 43	12.696	0.221	0.210	0.926	-0.031	11.612	0.252	
32	31.3	53 46	12.761	0.248	0.117	0.916	-0.033	11.554	0.281	B9.5 V	no RV	
33	25.3	53 45	12.691	0.236	0.112	0.749	-0.049	11.466	0.285	
34	21.0	53 03	12.577	0.280	-0.003	11.359	0.283*	Ap	...	
35	28.1	52 31	12.622	0.246	0.056	0.856	-0.038	11.399	0.284	
36	33.0	54 11	12.881	0.238	0.131	0.813	-0.043	11.675	0.281	
37	27.5	53 14	12.881	0.232	0.124	0.911	-0.033	11.742	0.265	
38	27.3	51 29	12.761	0.237	0.136	0.855	-0.038	11.577	0.275	A0 V	no RV	
39	31.5	55 14	13.360	0.241	0.116	0.856	-0.038	12.159	0.279	
40	39.5	53 40	13.272	0.153	0.248	0.785	-0.044	12.426	0.197	N
41	27.6	53 45	13.239	0.222	0.153	0.761	-0.047	12.081	0.269	
42	25.1	51 26	13.103	0.266	0.129	1.097	-0.015	11.895	0.281	
43	22.2	53 49	13.086	0.300	0.009	11.833	0.291*	A2 V	-2	N
44	21.9	53 53	13.236	0.294	0.002	11.980	0.292*	
45	26.2	52 56	13.304	0.289	0.010	12.103	0.279*	
46	23.4	52 51	13.215	0.333	0.053	12.012	0.280*	A4 V	-14	?
47	26.6	52 55	13.526	0.311	0.032	12.327	0.279*	
48	37.5	53 38	13.411	0.273	0.311	0.842	-0.040	12.063	0.313	
49	26.8	53 22	13.666	0.301	0.017	12.446	0.284*	F8 V	-13	?
50	23.9	53 34	14.009	0.357	0.069	12.772	0.288*	
	25.5	55 58	10.508	0.574	0.260	9.159	0.314*	K2 III	-1	N
	26.8	53 43	11.026	0.263	0.054	0.495	-0.075	9.575	0.338	B5 V	-23	= Hayford 7
	05.1	50 10	11.397	0.362	0.102	10.280	0.260*	
	49.3	54 40	11.460	0.362	0.409	0.912	-0.035	9.752	0.397*	N
	22.6	50 16	11.674	0.184	0.043	0.725	-0.050	10.667	0.234	
	23.0	58 20	11.928	0.333	0.191	0.514	-0.074	10.178	0.407*	N
	26.8	53 48	12.082	0.261	0.052	0.587	-0.065	10.679	0.326	B6 V	-13	= Hayford 7A
	24.2	54 08	12.346	0.254	0.039	0.664	-0.058	11.006	0.312	B7.5 V	-22	

TABLE 1—Continued

Zug No.	RA	dec	V	(b-y)	m_1	c_1	$(b - y)_o$	V_o	$E(b - y)^a$	Sp T	RV	Notes ^b
24.0	54 12	12.393	0.285	-0.010	11.127	0.295*	
41.0	48 49	12.443	0.242	0.224	0.962	...	-0.028	11.282	0.270	
36.9	52 12	12.479	0.419	0.154	11.339	0.265*	
07.6	56 09	12.618	0.407	0.082	11.219	0.325*	
40.5	48 47	12.637	0.154	0.141	0.710	...	-0.051	11.755	0.205	
04.9	51 29	12.690	0.191	0.135	0.862	...	-0.037	11.710	0.228	
28.7	50 15	12.692	0.361	0.113	11.627	0.248*	
22.5	48 46	12.768	0.224	0.191	1.014	...	-0.022	11.708	0.246*	
20.6	57 28	12.793	1.288	N
33.6	49 20	12.812	0.154	0.141	0.859	...	-0.036	11.993	0.190	
39.9	56 19	12.814	0.241	0.506	0.273	...	-0.096	11.365	0.337*	
24.1	51 24	12.893	0.223	0.087	0.911	...	-0.033	11.794	0.256	
27.8	51 57	12.975	0.242	0.106	0.939	...	-0.030	11.805	0.272	
06.1	54 37	12.978	0.307	-0.002	11.649	0.309*	
24.3	51 34	12.985	0.255	0.099	1.026	...	-0.022	11.795	0.277	
25.2	56 58	13.032	0.814	N
42.2	54 44	13.039	0.727	0.436	...	11.790	0.291*	
13.5	57 21	13.045	1.186	N
27.8	58 30	13.101	0.212	0.292	0.540	...	-0.069	11.892	0.281*	
30.6	49 59	13.233	0.389	0.145	...	12.185	0.244*	
25.6	52 07	13.250	1.125	N
30.2	50 13	13.285	0.338	0.092	...	12.225	0.246*	
39.7	50 08	13.297	0.148	0.179	0.868	...	-0.035	12.509	0.183	
16.8	53 02	13.330	0.246	0.089	0.977	...	-0.027	12.158	0.273	
16.8	53 51	13.357	0.417	0.122	...	12.090	0.295*	
21.7	50 53	13.414	0.265	0.076	0.968	...	-0.028	12.155	0.293	
13.4	50 40	13.417	0.637	0.376	...	12.296	0.261*	
17.3	50 36	13.434	0.393	0.135	...	12.325	0.258*	
20.2	50 34	13.437	0.333	0.077	...	12.336	0.256*	
21.9	55 40	13.443	0.302	-0.010	...	12.101	0.312*	
22.3	54 44	13.451	0.284	-0.017	...	12.155	0.301*	
46.4	56 36	13.465	0.166	0.290	0.839	...	-0.039	12.585	0.205*	N
16.8	53 54	13.476	0.401	0.106	...	12.206	0.295*	
38.8	55 26	13.492	0.355	0.419	0.191	...	-0.106	11.508	0.461*	N
24.1	53 06	13.498	0.824	N
26.0	52 23	13.515	0.210	0.130	0.862	...	-0.037	12.452	0.247	
21.0	51 31	13.517	0.254	0.100	1.003	...	-0.024	12.321	0.278	
23.4	50 13	13.517	0.173	0.177	0.956	...	-0.027	12.656	0.200*	
32.5	50 50	13.604	0.367	0.115	...	12.519	0.252*	
24.6	55 25	13.611	0.262	0.199	0.888	...	-0.036	12.331	0.298	
31.0	51 44	13.639	0.213	0.176	0.911	...	-0.032	12.584	0.245	
25.1	52 15	13.657	0.280	0.008	...	12.487	0.272*	
15.6	52 45	13.671	0.260	0.144	0.951	...	-0.029	12.427	0.289	
10.7	50 06	13.675	0.516	0.260	...	12.574	0.256*	
09.7	51 23	13.704	0.361	0.090	...	12.539	0.271*	
25.7	51 54	13.710	0.317	0.049	...	12.558	0.268*	
19.3	54 40	13.714	0.399	0.097	...	12.414	0.302*	
17.1	56 52	13.722	0.311	-0.017	...	12.310	0.328*	
31.8	56 35	13.733	0.395	0.078	...	12.370	0.317*	
35.4	52 59	13.753	0.736	N
25.1	52 39	13.776	0.342	0.065	...	12.587	0.277*	
14.3	55 49	13.783	0.357	0.039	...	12.415	0.318*	
26.4	52 35	13.818	0.260	0.125	1.031	...	-0.021	12.608	0.281*	
33.0	52 50	13.824	0.222	0.192	0.896	...	-0.034	12.723	0.256*	
36.3	54 17	13.833	0.258	0.203	0.892	...	-0.035	12.572	0.293	
23.9	53 01	13.833	0.415	0.134	...	12.623	0.281*	
35.8	53 24	13.837	0.202	0.249	0.851	...	-0.038	12.805	0.240*	
29.5	52 42	13.841	0.241	0.115	1.032	...	-0.021	12.715	0.262*	
14.0	55 47	13.846	0.862	0.544	...	12.479	0.318*	

TABLE 1—Continued

Zug No.	RA	dec	V	(b-y)	m_1	c_1	$(b - y)_o$	V_o	$E(b - y)^a$	Sp T	RV	Notes ^b
22.7	52 23	13.865	0.934	N
24.4	51 40	13.878	0.276	0.124	1.024	-0.022	12.595	0.298*	
23.7	57 03	13.885	0.419	0.092	12.480	0.327*	
36.8	53 30	13.891	0.207	0.248	0.881	-0.035	12.849	0.242*	
13.2	51 23	13.896	0.317	0.048	12.740	0.269*	
21.4	50 31	13.897	0.260	0.205	0.944	-0.030	12.650	0.290*	
13.9	54 53	13.914	0.598	0.290	12.590	0.308*	
23.2	52 23	13.920	0.280	0.005	12.738	0.275*	
04.6	53 27	13.924	0.351	0.054	12.648	0.297*	
09.8	51 47	13.961	0.367	0.092	12.777	0.275*	
06.1	55 43	13.964	0.371	0.050	12.582	0.321*	
45.3	55 03	13.973	0.290	0.287	0.738	-0.051	12.507	0.341*	N
20.5	57 13	13.975	0.399	0.069	12.554	0.330*	
08.5	52 50	13.991	0.328	0.040	12.754	0.288*	
22.5	51 41	13.993	0.328	0.061	12.844	0.267*	A7 V	-14	N	
26.2	54 37	14.004	0.336	0.038	12.723	0.298*	
39.6	52 24	14.009	0.449	0.183	12.866	0.266*	
17.8	53 42	14.014	0.401	0.109	12.757	0.292*	
46.7	50 25	14.024	0.221	0.317	0.700	-0.053	12.844	0.274*	
31.3	53 09	14.036	0.424	0.145	12.837	0.279*	
19.8	52 39	14.048	0.265	0.146	1.041	-0.021	12.820	0.286*	
37.3	53 13	14.053	0.343	0.067	12.865	0.276*	
32.5	52 37	14.069	0.399	0.127	12.898	0.272*	
20.7	54 32	14.085	0.798	N
27.5	53 09	14.131	0.265	0.144	1.028	-0.022	12.898	0.287*	
28.8	51 31	14.131	0.327	0.065	13.005	0.262*	
17.7	48 34	14.138	0.739	N
06.1	53 15	14.151	0.452	0.158	12.888	0.294*	
22.9	51 53	14.164	0.272	0.151	1.026	-0.022	12.899	0.294*	
38.2	53 45	14.170	0.237	0.283	0.813	-0.043	12.968	0.280*	
09.8	52 32	14.170	1.039	N
26.2	53 53	14.181	0.896	N
36.0	52 17	14.186	0.250	0.187	0.969	-0.027	12.993	0.277*	
24.7	54 46	14.199	1.173	N
44.3	49 32	14.200	0.915	N
15.2	57 43	14.202	0.500	0.161	12.745	0.339*	
11.0	52 26	14.204	0.349	0.067	12.992	0.282*	
07.4	50 47	14.216	0.340	0.075	13.075	0.265*	
44.0	52 46	14.227	1.386	N
30.1	53 20	14.235	0.817	N
41.0	48 28	14.235	0.718	0.497	13.284	0.221*	
06.9	50 49	14.236	1.092	N
17.8	55 08	14.241	0.434	0.126	12.915	0.308*	
32.9	51 46	14.247	0.662	0.400	13.118	0.262*	
20.2	54 23	14.256	1.252	N
30.4	50 30	14.263	0.890	N
33.0	52 46	14.273	0.297	0.023	13.097	0.274*	
17.7	57 10	14.280	0.373	0.042	12.856	0.331*	
46.0	50 41	14.303	0.434	0.191	13.258	0.243*	
45.9	50 35	14.304	0.236	0.254	0.897	-0.034	13.142	0.270*	
39.7	49 35	14.324	0.440	0.206	13.317	0.234*	
16.9	54 55	14.342	0.335	0.029	13.024	0.306*	
16.8	50 44	14.343	0.348	0.088	13.226	0.260*	
08.5	54 22	14.346	0.338	0.033	13.035	0.305*	
30.3	53 29	14.354	0.286	0.003	13.136	0.283*	
30.6	52 50	14.367	0.286	0.010	13.182	0.276*	A8 V	no RV	...	
24.9	51 18	14.368	0.296	0.034	13.243	0.262*	
21.0	57 52	14.380	1.294	N
29.7	51 56	14.386	0.294	0.028	13.241	0.266*	

TABLE 1—Continued

Zug No.	RA	dec	V	(b-y)	m_1	c_1	$(b - y)_o$	V_o	$E(b - y)^a$	Sp T	RV	Notes ^b
32.8	50 41	14.390	0.454	0.204	13.313	0.250*	
46.8	49 55	14.403	0.339	0.105	13.396	0.234*	
11.3	55 31	14.411	0.367	0.051	13.051	0.316*	
41.9	49 20	14.457	0.269	0.198	0.84	-0.040	13.129	0.309*	
07.5	50 03	14.459	0.411	0.154	13.353	0.257*	
27.8	53 40	14.478	0.357	0.071	13.246	0.286*	
38.4	51 28	14.479	0.266	0.275	0.775	-0.047	13.134	0.313*	
25.1	53 21	14.480	0.291	0.007	13.257	0.284*	F6 III	-5	N	
26.0	54 26	14.482	0.404	0.108	13.208	0.296*	
48.5	50 00	14.492	0.391	0.157	13.485	0.234*	
10.6	49 24	14.493	1.040	N
13.5	54 23	14.514	0.420	0.118	13.213	0.302*	
34.1	54 03	14.518	0.415	0.128	13.282	0.287*	
19.9	53 21	14.534	0.318	0.031	13.298	0.287*	
13.6	51 22	14.534	0.332	0.063	13.379	0.269*	
12.1	55 52	14.535	0.497	0.177	13.160	0.320*	
49.3	49 33	14.544	1.184	N
25.7	53 26	14.545	0.407	0.122	13.319	0.285*	
15.1	52 47	14.549	0.340	0.056	13.329	0.284*	
19.5	53 27	14.550	0.373	0.084	13.308	0.289*	
36.7	54 25	14.551	0.315	0.025	13.304	0.290*	
27.3	53 11	14.553	0.381	0.100	13.343	0.281*	
21.2	56 27	14.561	0.391	0.070	13.179	0.321*	
16.6	55 01	14.565	0.406	0.098	13.242	0.308*	
35.8	49 25	14.587	0.899	N
33.0	53 33	14.597	0.324	0.042	13.383	0.282*	
11.2	56 44	14.598	0.328	-0.002	13.179	0.330*	
04.7	55 18	14.602	0.391	0.074	13.237	0.317*	
29.7	52 51	14.602	1.055	N
27.6	51 32	14.611	0.503	0.240	13.481	0.263*	
17.6	53 09	14.620	0.369	0.083	13.389	0.286*	
36.4	48 36	14.622	0.389	0.164	13.654	0.225*	
46.1	53 17	14.645	1.099	N
33.6	53 37	14.672	1.398	N
36.2	52 19	14.673	0.425	0.158	13.526	0.267*	
29.4	54 08	14.678	0.328	0.037	13.427	0.291*	
23.9	53 44	14.687	0.371	0.081	13.442	0.290*	
16.4	53 28	14.698	0.389	0.099	13.449	0.290*	
39.4	51 04	14.710	0.792	N
11.4	53 29	14.711	0.834	N
35.5	49 35	14.717	0.575	0.338	13.700	0.237*	
28.2	52 02	14.723	0.376	0.108	13.571	0.268*	
28.2	52 18	14.730	0.396	0.125	13.564	0.271*	
03.9	50 07	14.732	0.347	0.087	13.614	0.260*	
16.8	58 30	14.738	0.502	0.155	13.247	0.347*	
23.9	55 34	14.741	1.288	N
41.6	51 46	14.744	0.532	0.274	13.636	0.258*	
17.6	57 52	14.752	0.402	0.063	13.294	0.339*	
35.1	52 37	14.769	0.429	0.158	13.604	0.271*	
08.8	56 28	14.776	0.591	0.263	13.364	0.328*	
38.9	52 22	14.778	0.415	0.149	13.635	0.266*	
20.7	58 00	14.782	0.888	N
21.3	55 49	14.784	0.478	0.164	13.433	0.314*	
29.5	55 50	14.788	0.912	N
33.9	48 58	14.791	0.371	0.140	13.800	0.231*	
46.6	51 03	14.792	0.476	0.229	13.730	0.247*	
21.6	57 15	14.795	1.207	N
21.7	50 20	14.795	0.400	0.147	13.709	0.253*	
25.1	55 16	14.796	0.245	0.544	0.671	-0.057	13.498	0.302*

TABLE 1—Continued

Zug No.	RA	dec	V	(b-y)	m_1	c_1	$(b - y)_o$	V_o	$E(b - y)^a$	Sp	T	RV	Notes ^b
39.4	50 08	14.799	0.758	
03.8	54 05	14.801	1.596	N
22.9	49 53	14.807	0.436	0.189	13.746	0.247*	
31.5	52 12	14.809	0.352	0.084	13.657	0.268*	
16.2	56 51	14.813	1.231	N
34.9	51 38	14.821	0.359	0.099	13.704	0.260*	
09.1	54 07	14.837	0.378	0.076	13.539	0.302*	
21.7	53 32	14.838	0.403	0.115	13.598	0.288*	
41.3	53 02	14.847	0.898	N
28.3	54 41	14.858	0.361	0.063	13.578	0.298*	
15.4	49 33	14.858	0.791	N
20.8	56 50	14.862	0.859	N
31.3	49 20	14.862	0.424	0.188	13.847	0.236*	
26.8	52 37	14.870	1.449	N
31.5	49 12	14.882	0.897	N
35.0	50 35	14.888	0.444	0.196	13.821	0.248*	
39.9	51 47	14.891	0.391	0.132	13.778	0.259*	
36.6	53 29	14.906	0.917	N
32.4	52 42	14.908	0.482	0.209	13.733	0.273*	
11.3	55 11	14.915	0.538	0.225	13.571	0.313*	
33.4	48 52	14.921	0.419	0.189	13.934	0.230*	
11.8	48 50	14.947	0.897	N
49.0	50 50	14.948	0.362	0.119	13.903	0.243*	
33.1	54 04	14.953	1.078	N
37.8	52 56	14.962	0.399	0.126	13.788	0.273*	
23.7	51 17	14.966	0.860	N
28.6	54 08	14.970	0.334	0.043	13.717	0.291*	
10.4	55 33	14.986	0.503	0.186	13.622	0.317*	
38.7	49 43	15.001	1.138	N
02.4	54 30	15.009	0.553	0.243	13.677	0.310*	
11.0	54 00	15.009	1.308	N
37.6	54 53	15.010	0.397	0.102	13.742	0.295*	
18.8	57 31	15.011	0.884	N
25.0	49 58	15.030	0.537	0.290	13.970	0.247*	
43.6	49 29	15.030	1.277	N
16.9	52 13	15.030	0.505	0.229	13.842	0.276*	
40.2	55 46	15.032	1.084	N
23.7	51 53	15.033	1.050	N
45.8	51 11	15.046	0.490	0.241	13.976	0.249*	
41.3	51 15	15.050	0.328	0.076	13.966	0.252*	
36.9	49 52	15.071	1.201	N
30.2	52 23	15.086	0.447	0.176	13.922	0.271*	
49.0	51 12	15.093	0.404	0.157	14.030	0.247*	
35.2	48 18	15.096	0.618	0.396	14.140	0.222*	
45.6	52 01	15.106	0.974	N
14.5	52 11	15.112	0.436	0.159	13.920	0.277*	
25.3	54 42	15.126	0.528	0.229	13.839	0.299*	
43.9	52 42	15.127	0.820	N
22.8	53 45	15.137	0.395	0.105	13.889	0.290*	
22.5	50 36	15.142	0.457	0.202	14.045	0.255*	
22.8	54 27	15.145	0.439	0.141	13.863	0.298*	
32.1	54 08	15.166	0.408	0.118	13.921	0.290*	
24.2	52 43	15.183	0.410	0.132	13.988	0.278*	
30.9	50 35	15.187	0.916	N
28.3	54 08	15.188	0.405	0.114	13.935	0.291*	
28.8	51 41	15.195	1.428	N
15.1	49 21	15.197	0.578	0.333	14.143	0.245*	
13.9	57 14	15.199	0.407	0.073	13.762	0.334*	
34.0	53 42	15.201	0.969	N

TABLE 1—Continued

Zug No.	RA	dec	V	(b-y)	m_1	c_1	$(b - y)_o$	V_o	$E(b - y)^a$	Sp	T	RV	Notes ^b
11.2	53 39	15.210	0.552	0.257	13.940	0.295*	
22.6	51 16	15.210	0.391	0.128	14.081	0.263*	
10.5	56 02	15.220	1.289	N
38.5	50 26	15.248	1.334	N
11.2	51 58	15.263	0.610	0.333	14.074	0.277*	
33.6	54 06	15.263	0.447	0.159	14.024	0.288*	
14.2	56 39	15.264	0.453	0.125	13.856	0.328*	
24.0	52 47	15.269	0.424	0.145	14.070	0.279*	
30.0	56 24	15.274	0.516	0.200	13.915	0.316*	
35.0	54 46	15.280	0.638	0.343	14.012	0.295*	
34.6	50 23	15.281	0.489	0.243	14.223	0.246*	
11.9	56 17	15.281	1.118	N
23.5	54 07	15.283	0.458	0.164	14.019	0.294*	
28.3	50 31	15.283	0.980	N
15.0	51 52	15.296	1.048	N
19.6	53 01	15.306	0.400	0.116	14.086	0.284*	
27.0	53 13	15.308	1.461	N
44.5	49 05	15.323	0.450	0.224	14.351	0.226*	
13.2	48 59	15.325	0.423	0.181	14.284	0.242*	
07.9	55 20	15.326	0.614	0.298	13.966	0.316*	
34.6	52 44	15.330	0.413	0.141	14.159	0.272*	
42.1	50 18	15.330	0.457	0.216	14.294	0.241*	
12.6	51 19	15.339	0.526	0.257	14.184	0.269*	
33.0	55 04	15.342	0.951	N
05.9	54 24	15.354	0.931	N
32.5	52 54	15.365	0.936	N
23.3	51 04	15.380	0.560	0.300	14.262	0.260*	
43.1	50 25	15.382	0.365	0.123	14.342	0.242*	
31.8	56 42	15.384	0.975	N
11.6	55 43	15.386	1.175	N
25.6	54 22	15.390	0.946	N
13.9	56 38	15.395	0.910	N
43.5	50 11	15.403	0.567	0.328	14.375	0.239*	
31.5	56 06	15.406	0.458	0.146	14.065	0.312*	
44.0	54 00	15.407	1.004	N
03.3	55 03	15.419	0.523	0.207	14.062	0.316*	
20.9	53 42	15.419	0.558	0.267	14.169	0.291*	
36.7	52 40	15.434	0.500	0.230	14.271	0.270*	
37.8	54 17	15.442	0.473	0.185	14.204	0.288*	
43.9	52 39	15.444	0.458	0.192	14.299	0.266*	
11.1	55 28	15.445	0.511	0.195	14.087	0.316*	
31.0	48 51	15.459	0.526	0.295	14.466	0.231*	
20.2	49 56	15.472	0.408	0.159	14.402	0.249*	
24.5	50 32	15.480	1.009	N
29.6	51 25	15.484	0.475	0.215	14.364	0.260*	
22.1	50 46	15.493	0.931	N
47.8	51 37	15.498	0.516	0.263	14.412	0.253*	
10.7	52 25	15.507	0.456	0.174	14.295	0.282*	
41.4	50 23	15.508	0.629	0.387	14.466	0.242*	
09.9	52 56	15.511	0.512	0.224	14.272	0.288*	
12.7	54 03	15.513	0.645	0.346	14.227	0.299*	
18.6	50 26	15.514	0.949	N
18.9	54 47	15.520	0.952	N
07.8	56 24	15.529	0.592	0.264	14.118	0.328*	
27.8	53 12	15.530	0.437	0.156	14.321	0.281*	
29.9	55 21	15.531	0.599	0.295	14.223	0.304*	
07.8	56 35	15.536	0.551	0.221	14.117	0.330*	
26.3	51 59	15.541	0.622	0.354	14.387	0.268*	
43.6	52 26	15.544	0.548	0.284	14.408	0.264*	

TABLE 1—Continued

Zug No.	RA	dec	V	(b-y)	m_1	c_1	$(b - y)_o$	V_o	$E(b - y)^a$	Sp T	RV	Notes ^b
45.9	51 28	15.545	1.009	N
28.3	50 54	15.550	0.522	0.267	14.453	0.255*	
30.2	51 36	15.554	0.960	N
40.1	54 33	15.561	0.487	0.197	14.315	0.290*	
26.2	52 31	15.567	1.048	N
39.6	51 09	15.567	0.427	0.175	14.484	0.252*	
31.8	48 52	15.568	0.690	0.459	14.576	0.231*	
23.1	54 40	15.572	0.976	N
38.9	53 34	15.574	0.717	N
09.2	55 15	15.574	0.487	0.173	14.222	0.314*	
11.2	55 19	15.575	0.600	0.286	14.224	0.314*	
05.3	50 58	15.576	0.530	0.261	14.421	0.269*	
15.5	53 36	15.582	0.479	0.186	14.324	0.293*	
21.7	52 25	15.588	0.405	0.129	14.401	0.276*	
25.9	55 00	15.592	0.608	0.306	14.291	0.302*	
12.1	52 40	15.597	1.207	N
46.9	51 14	15.602	0.546	0.297	14.532	0.249*	
22.3	51 27	15.606	0.486	0.221	14.468	0.265*	
45.4	49 39	15.621	0.497	0.265	14.624	0.232*	
23.4	53 26	15.622	0.460	0.174	14.390	0.286*	
45.2	51 04	15.626	1.175	N
13.4	51 42	15.639	0.505	0.233	14.468	0.272*	
12.1	53 39	15.646	0.433	0.138	14.378	0.295*	
29.4	51 13	15.652	0.535	0.277	14.541	0.258*	
11.4	52 12	15.671	0.945	N
22.7	52 17	15.675	0.916	N
36.6	50 38	15.678	0.472	0.224	14.613	0.248*	
40.8	51 31	15.683	0.573	0.318	14.585	0.255*	
42.0	50 59	15.683	0.602	0.353	14.614	0.249*	
19.7	50 34	15.704	1.439	N
06.7	55 39	15.709	0.567	0.247	14.332	0.320*	
17.5	52 20	15.711	0.482	0.205	14.519	0.277*	
33.5	52 54	15.714	0.975	N
07.1	54 16	15.715	1.289	N
30.7	51 41	15.716	0.526	0.263	14.586	0.263*	
33.7	55 19	15.721	0.584	0.282	14.423	0.302*	
38.0	50 27	15.731	0.460	0.215	14.678	0.245*	
08.7	57 16	15.732	0.507	0.170	14.282	0.337*	
39.1	51 22	15.736	0.474	0.219	14.642	0.255*	
36.7	55 11	15.739	0.533	0.234	14.455	0.299*	
46.7	52 53	15.745	0.940	N
37.9	54 06	15.752	0.531	0.245	14.523	0.286*	
25.3	50 51	15.762	0.484	0.228	14.660	0.256*	
27.3	51 53	15.768	0.538	0.271	14.620	0.267*	
25.3	53 51	15.775	0.556	0.266	14.528	0.290*	
24.5	54 34	15.776	0.936	N
25.8	51 41	15.781	0.683	0.418	14.640	0.265*	
36.2	53 21	15.793	1.141	N
25.4	51 59	15.797	0.509	0.240	14.640	0.269*	
15.4	54 47	15.804	0.534	0.228	14.489	0.306*	
17.3	57 37	15.812	0.473	0.136	14.365	0.337*	
18.7	55 44	15.823	0.497	0.182	14.470	0.315*	
31.6	51 40	15.825	1.091	N
29.5	54 51	15.827	0.617	0.318	14.542	0.299*	
26.8	55 35	15.828	0.529	0.220	14.501	0.309*	
34.9	51 53	15.830	1.290	N
28.1	51 51	15.832	0.656	0.390	14.688	0.266*	
29.0	55 17	15.841	0.632	0.328	14.534	0.304*	
47.6	51 09	15.852	0.535	0.288	14.788	0.247*	

TABLE 1—Continued

Zug No.	RA	dec	V	(b-y)	m_1	c_1	$(b - y)_o$	V_o	$E(b - y)^a$	Sp T	RV	Notes ^b
20.4	55 30	15.852	1.230	N
12.0	50 52	15.855	0.935	N
15.2	51 54	15.857	0.516	0.242	14.681	0.274*	
34.1	50 52	15.879	0.454	0.202	14.797	0.252*	
10.1	53 49	15.891	0.508	0.210	14.610	0.298*	
07.9	51 54	15.893	0.982	N
46.8	52 21	15.914	0.454	0.193	14.790	0.261*	
19.4	49 25	15.932	0.988	N
20.6	52 27	15.940	0.538	0.261	14.750	0.277*	
35.7	54 38	15.941	0.434	0.141	14.681	0.293*	
29.6	54 10	15.950	0.489	N
15.5	51 07	15.955	0.521	0.256	14.817	0.265*	
25.5	51 46	15.960	0.503	0.236	14.814	0.267*	
21.3	52 11	15.967	0.657	0.384	14.791	0.273*	
40.7	53 49	15.969	0.739	0.458	14.760	0.281*	
32.7	54 28	15.975	0.518	0.225	14.716	0.293*	
36.2	50 20	15.984	0.409	0.164	14.932	0.245*	
11.6	53 48	15.984	0.551	0.254	14.707	0.297*	
34.4	52 57	15.991	0.558	0.283	14.809	0.275*	
22.2	52 26	15.993	0.547	0.271	14.807	0.276*	
32.0	51 46	15.996	0.496	0.233	14.866	0.263*	
14.5	51 51	15.999	0.584	0.311	14.823	0.273*	
40.8	54 25	16.006	0.507	0.219	14.768	0.288*	
13.7	52 47	16.017	0.451	N
16.9	52 17	16.022	0.577	0.300	14.831	0.277*	
19.2	54 26	16.025	0.650	0.350	14.736	0.300*	
18.3	54 25	16.035	0.594	0.294	14.744	0.300*	
36.2	51 54	16.035	0.646	0.384	14.908	0.262*	
39.9	54 48	16.037	0.706	N
07.9	53 09	16.038	0.707	0.415	14.784	0.292*	
12.6	53 56	16.044	0.552	0.254	14.763	0.298*	
36.7	54 29	16.052	0.581	0.290	14.801	0.291*	
11.1	54 49	16.055	0.758	N
15.7	51 20	16.062	0.463	0.196	14.914	0.267*	
26.5	50 58	16.074	0.518	0.261	14.969	0.257*	
20.8	53 59	16.079	0.504	0.210	14.815	0.294*	
12.4	53 57	16.090	0.567	0.269	14.808	0.298*	
11.4	50 52	16.094	0.494	0.230	14.958	0.264*	
27.9	50 01	16.114	0.550	0.304	15.058	0.246*	
25.5	50 58	16.122	0.978	N
33.5	54 20	16.134	0.510	0.219	14.883	0.291*	
20.0	51 41	16.142	0.573	0.304	14.987	0.269*	
10.9	52 08	16.151	0.735	0.456	14.953	0.279*	
12.6	52 52	16.167	0.890	N
09.1	51 14	16.172	0.622	0.352	15.013	0.270*	
34.6	53 58	16.175	0.684	0.398	14.944	0.286*	
25.8	51 14	16.212	1.042	N
44.9	52 31	16.221	0.498	0.234	15.085	0.264*	
13.6	50 13	16.228	0.506	0.250	15.129	0.256*	
40.8	50 32	16.234	0.587	0.343	15.184	0.244*	
15.3	53 06	16.247	0.678	0.391	15.012	0.287*	
33.9	52 54	16.311	0.687	0.412	15.130	0.275*	
39.1	51 27	16.313	0.610	0.354	15.214	0.256*	
16.2	51 55	16.332	0.508	0.235	15.157	0.273*	
14.2	52 19	16.374	0.566	0.287	15.175	0.279*	
31.1	54 09	16.376	0.576	0.286	15.128	0.290*	

NOTE.—Table 1 is published here in its entirety. In cases where the IRAF formal errors are large for m_1 and c_1 , values have been dropped.

^aThe * indicates extinction found from fit to B star extinctions. See section 3.1.

^bN means likely not a cluster member; see section 3.3.

A. Photometry Calibration Details

In order to document the data reduction process which produced the photometry in this table, the following material is included. Table 2 lists the Strömgren standard stars used for the PE photometry and their properties. Table 3 lists the Strömgren magnitudes and colors derived from the PE photometry for stars in the area of the cluster.

The transformation equations to standard magnitudes and colors for the PE photometry (values from 6/29/1997; other nights are similar):

$y = \text{mag1} + (0.6204 \pm 0.0098) + (0.0327 \pm 0.0078)(\text{mag2-mag1}) - (0.1382 \pm 0.0072)\text{X1}$	stdev = 0.0058
$(b-y) = (\text{mag2-mag1}) + (0.0321 \pm 0.0101) + (0.0778 \pm 0.0082)(\text{mag2-mag1}) - (0.0596 \pm 0.0070)\text{X2}$	stdev = 0.0050
$m1 = (\text{mag3-mag2}) - (\text{mag2-mag1}) + (0.1243 \pm 0.0108) - (0.1186 \pm 0.0091)(\text{mag2-mag1}) - (0.0613 \pm 0.0076)\text{X3}$	stdev = 0.0123
$c1 = (\text{mag4-mag3}) - (\text{mag3-mag2}) + (0.9481 \pm 0.0259) + (0.2222 \pm 0.0186)(\text{mag2-mag1}) - (0.1364 \pm 0.0177)\text{X4}$	stdev = 0.0313

The transformation equations to standard magnitudes for the CCD photometry are:

$\text{mag1} = y + (4.3396 \pm 0.0294) - (0.0070 \pm 0.0634)\text{by}$	stdev = 0.0965
$\text{mag2} = (\text{by} + y) + (4.4062 \pm 0.0256) + (0.2001 \pm 0.1094)\text{by}$	stdev = 0.0661
$\text{mag3} = \text{im1} + 2*\text{by} + y + (5.1438 \pm 0.0305) + (0.1763 \pm 0.1418)\text{by}$	stdev = 0.0623
$\text{mag4} = \text{c1} + 2*\text{m1} + 2*\text{by} + y + (5.7482 \pm 0.2119) + (0.2221 \pm 0.2119)\text{by}$	stdev = 0.0976

TABLE 2
STANDARD STARS USED FOR PHOTOELECTRIC PHOTOMETRY OF NGC6520

Star	V	ΔV	$(b - y)$	$\Delta(b - y)$	m1	$\Delta m1$	c1	$\Delta c1$	night ^a
BD043508	9.326	0.02	1.178	0.02	INDEF	INDEF	INDEF	INDEF	123--
HD110184	8.297	0.01	0.818	0.01	0.163	0.01	0.707	0.01	123--
HD119537	6.518	0.02	0.029	0.02	0.172	0.02	0.983	0.02	---45
HD120086	7.872	0.02	-0.083	0.02	0.098	0.02	0.15	0.02	---45
HD123825	7.254	0.02	0.984	0.02	0.792	0.02	0.395	0.02	123--
HD126273	7.190	0.02	1.063	0.02	0.639	0.02	0.577	0.02	123--
HD129956	5.685	0.02	0.005	0.02	0.120	0.02	1.023	0.02	---4-
HD131597	8.429	0.01	0.473	0.01	0.206	0.01	0.303	0.01	123--
HD136831	6.291	0.02	0.008	0.02	0.136	0.02	1.102	0.02	---4-
HD140850	8.816	0.02	1.102	0.02	INDEF	INDEF	INDEF	INDEF	123--
HD145774	7.484	0.02	-0.021	0.02	0.062	0.02	0.076	0.02	---4-
HD154345	6.771	0.02	0.449	0.02	0.270	0.02	0.286	0.02	123--
HD160233	9.095	0.02	0.025	0.02	0.032	0.02	0.071	0.02	---45
HD160314	7.730	0.02	0.273	0.02	0.161	0.02	0.638	0.02	123--
HD160315	6.260	0.02	0.642	0.02	0.392	0.02	0.452	0.02	123--
HD161573	6.847	0.02	0.060	0.02	0.052	0.02	0.346	0.02	---45
HD161817	6.982	0.01	0.137	0.01	0.113	0.01	1.206	0.01	123--
HD162596	6.342	0.02	0.717	0.02	0.376	0.02	0.429	0.02	123--
HD165401	6.801	0.01	0.393	0.01	0.166	0.01	0.288	0.01	123--
HD165462	6.346	0.02	0.700	0.02	0.279	0.02	0.552	0.02	123--
HD169578	6.730	0.02	0.049	0.02	0.073	0.02	0.860	0.02	123--
HD172365	6.369	0.02	0.510	0.02	0.226	0.02	0.701	0.02	123--
HD172829	8.460	0.02	1.389	0.02	INDEF	INDEF	INDEF	INDEF	123--
HD174240	6.235	0.02	0.037	0.02	0.131	0.02	1.112	0.02	123--
HD176582	6.420	0.02	-0.068	0.02	0.094	0.02	0.260	0.02	1234-
HD190299	5.670	0.02	0.827	0.02	0.537	0.02	0.470	0.02	123--
HD198820	6.427	0.01	-0.053	0.01	0.097	0.01	0.364	0.01	-2345
HD199280	6.566	0.02	-0.031	0.02	0.109	0.02	0.777	0.02	---45
HD200340	6.498	0.02	-0.026	0.02	0.082	0.02	0.559	0.02	---5
HD208527	6.389	0.02	1.091	0.02	0.743	0.02	0.426	0.02	123--
HD210460	6.182	0.005	0.446	0.005	0.212	0.005	0.326	0.005	123--

NOTE.—The standard values were taken from the Astronomical Almanac 2003 published by the US Naval Observatory, Appendix ubvy and H-beta Standard Stars.

^aOn some nights repeat observations were made.

TABLE 3
CALIBRATED CLUSTER STARS FROM PHOTOELECTRIC PHOTOMETRY OF NGC6520

Zug No	V	ΔV^a	$(b - y)$	$\Delta(b - y)$	m1	$\Delta m1$	c1	$\Delta c1$
8	10.904	0.004	0.233	0.002	0.073	0.021	0.487	0.028
_b	10.538	0.016	0.701	0.018	0.470	0.073	0.323	0.118
6	10.601	0.012	0.229	0.005	0.026	0.015	0.504	0.024
1	9.064	0.014	0.049	0.005	0.161	0.035	1.012	0.020
3	8.883	0.006	1.144	0.008	0.712	0.028	0.187	0.040
4	8.908	0.015	1.052	0.023	0.550	0.039	0.149	0.020
2	9.020	0.005	0.503	0.021	0.111	0.030	1.167	0.022
10	11.155	0.040	0.214	0.026	0.065	0.040	0.470	0.004
16	11.311	0.068	0.528	0.018	0.204	0.045	0.444	0.022
17	11.752	0.020	0.290	0.020	0.022	0.065	0.654	0.067
11	11.306	0.023	0.303	0.019	0.017	0.037	0.586	0.017
34	12.396	0.083	0.366	0.045	0.006	0.083	0.694	0.053
9	10.790	0.008	0.234	0.058	-0.033	0.103	0.754	0.067
5	10.210	0.006	0.194	0.008	-0.030	0.002	0.653	0.023
14	11.587	0.011	0.326	0.021	0.127	0.018	0.564	0.016
15	11.772	0.030	0.140	0.044	0.083	0.015	0.507	0.025
22	12.223	0.062	0.120	0.018	0.097	0.016	0.943	0.011
12	11.404	0.011	0.104	0.001	0.077	0.006	0.436	0.039
29	12.478	0.011	0.071	0.015	0.134	0.025	0.809	0.030
24	12.187	0.022	0.286	0.044	0.043	0.057	0.568	0.022
27	12.531	0.012	0.176	0.016	0.033	0.028	0.778	0.034
28	12.488	0.010	0.312	0.015	0.064	0.026	0.995	0.037

^aThe ΔV etc values are the standard deviation of a single observation from different nights.

^bThe Foreground K giant; RA 18 03 25.5 dec -27 55 58.